Master's Thesis

PCNA unloading is negatively regulated by BET proteins

Jinwoo Kim

Department of Biological Sciences

Graduate School of UNIST

2020

PCNA unloading is negatively regulated by BET proteins

Jinwoo Kim

Department of Biological Sciences

Graduate School of UNIST

PCNA unloading is negatively regulated by BET proteins

A thesis/dissertation
submitted to the Graduate School of UNIST
in partial fulfillment of the
requirements for the degree of
Master of Science

Jinwoo Kim

06/05/2020 of submission
Approved by

_____

Advisor
Kyungjae Myung

PCNA unloading is negatively regulated by BET proteins

Jinwoo Kim

This certifies that the thesis/dissertation of Jinwoo Kim is approved.

06/05/2020 of submission

_____

Advisor: Kyungjae Myung

_____

Jayil Lee

_____

Sukhyun Kang

ABSTRACT

Proliferating cell nuclear antigen (PCNA) is a DNA clamp essential for DNA replication. During DNA synthesis, PCNA is continuously loaded onto and unloaded from DNA. PCNA recruits various proteins to nascent DNA to facilitate chromosome duplication. Therefore, timely PCNA unloading is crucial for high-fidelity DNA replication. The ATAD5-RFC-like complex (ATAD5-RLC) unloads PCNA from replicated DNA. It is unclear how ATAD5-RLC activity is regulated to prevent premature PCNA unloading. Here, we found that BRD4, an acetyl-histone-binding chromatin reader, inhibits the PCNA-unloading activity of ATAD5-RLC. The BRD4 ET domain interacts with a region upstream of the ATAD5 PCNA-unloading domain. BRD4-ATAD5 binds to acetyl-histones in nascent chromatin. BRD4 released from chromatin correlates with PCNA unloading. Disruption of the interaction between BRD4 and acetyl-histones or between BRD4 and ATAD5 reduces the PCNA amount on chromatin. In contrast, the overexpression of BRD4 increases the amount of chromatin-bound PCNA. Thus, acetyl-histone-bound BRD4 fine-tunes PCNA unloading from nascent DNA.

TABLE OF CONTENTS

LIST OF FIGURES

LIST OF ABBREVIATIONS

PCNA	Proliferating cell nuclear antigen
TLS	Translesion synthesis
RFC	Replication factor C
RLC	RLC-like complex
CTF18	Chromosome transmission fidelity protein 18
ATAD5	ATPase family AAA domain-containing protein 5
BET	Bromo- and extra-terminal domain
BRD2, 3, 4	Bromodomain-containing protein 2, 3, 4
BD	Bromodomain
ET domain	Extra-terminal domain
P-TEFb	Positive transcription elongation factor b
TICRR	TOPBP1 interacting checkpoint and replication regulator
CMG	CDC45-MCM2-7-GINS
Elg1	Yeast homolog of ATAD5
Rtt106	Histone chaperone RTT106
iPOND	Isolation of proteins on nascent DNA
Edu	5-ethynyl-2´-deoxyuridine
AP-MS	Affinity purification mass spectrometry
NLS	Nuclear localization sequence
UAF1	Usp1-associated factor 1
H4K5Ac	The acetylation at the 5th lysine residue of the histone H4 protein
H4K12Ac	The acetylation at the 12th lysine residue of the histone H4 protein
MLV	Murine leukemia virus

NSD3	Histone-lysine N-methyltransferase
CHD4	Chromodomain-helicase-DNA-binding protein 4
CUPID	Cell-based unidentified protein interaction discovery
PKC-δ	Protein kinase C-δ
PMA	Phorbol-12-myristate 13-acetate
siRNA	Small interfering RNA
EU	5-ethynyl-uridine
JQ1	Thienotriazolodiazepine, BET bromodomain inhibitor
ATAD5 EK	ATAD5 (E1173K, EK)
BAH domain	Bromo adjacent homology domain
ORC1	Origin recognition complex 1
CTD	Carboxyl-terminal domain
JMJD6	Bifunctional arginine demethylase and lysyl-hydroxylase

1. Introduction

Eukaryotic DNA replication is tightly regulated for the accurate duplication of the genome (Kang et al., 2018). At replication fork, many replication factors cooperate for accurate genome duplication (Figure 1A). Proper association and dissociation of replication factors on replicating DNA are important for accurate replication initiation and termination.

Proliferating Cell Nuclear Antigen (PCNA) is a ring-structured DNA sliding clamp that tethers DNA polymerase to replicating DNA to enhance polymerase processivity (Figure 1B). PCNA functions as a molecular hub for replication and repair proteins (Moldovan et al., 2007). During DNA replication, PCNA interacts with various replication-related proteins such as a histone chaperone to facilitate nucleosome deposition (Shibahara and Stillman, 1999; Zhang et al., 2000) and a chromatin remodeler to assemble nascent chromatin (Poot et al., 2004). Upon replication machinery encounters DNA lesions, the lysine residue at position 164 of PCNA is subjected to mono-ubiquitination or poly-ubiquitination, which in turn recruits translesion synthesis (TLS) polymerase or triggers error-free lesion bypass, respectively (Chen et al., 2011).

PCNA ring encircles DNA and retention of PCNA on chromatin is regulated by three clamp-loader complexes: replication factor C (RFC) and two RFC-like complexes (RLCs) (Figure 2). Loading of PCNA onto primer-template junction is mediated by RFC and CTF18-RLC. ATAD5-RLC unloads PCNA (Kang et al., 2018, 2019). These three clamp loader complexes cooperate to contribute to genomic integrity and defects in any of them induce problem in cell cycle progression and replication rate. Importantly, PCNA must be removed from chromatin after DNA synthesis and repair. If not, persistent presence of PCNA on chromatin results in the inappropriate recruitment of replication proteins that causes genome instability (Lee et al., 2013) (Figure 3A). Therefore, PCNA unloading by ATAD5-RLC is crucial for maintaining genomic integrity, but it is unclear how the activity of ATAD5-RLC is regulated.

Chromatin assembly is tightly coupled with DNA replication (Kurat et al., 2017; Petryk et al., 2018; Reveron-Gomez et al., 2018; Yu et al., 2018). Parental nucleosomes are disassembled ahead of replicative helicase. Behind the replication fork, newly synthesized DNA strands are organized into nucleosome. Disassembled parental histones are transferred to newly replicated DNA. In addition, additional histones have to be synthesized to organize another nucleosome. In human cells, newly incorporated histones are marked by acetylation at K5 and K12 of histone H4 (Loyola et al., 2006; Sobel et al., 1995).

Histone acetylation or methylation are identified by chromatin reader proteins. These proteins recognize specific histone codes and assemble effectors to the chromatin. BET family proteins, such

as BRD2, BRD3 and BRD4, are representative chromatin readers that distinctively recognize acetylated histones by two bromodomains (BDs). BET proteins have an additional conserved domain called the extra-terminal (ET) domain. ET domains enable BET proteins to interact with a wide range of effector molecules that regulate transcription, DNA replication and repair (Donati et al., 2018).

As one of BET proteins, BRD4 is a well-known transcription regulator for diverse essential genes. BRD4 binds to histone modifiers and chromatin remodelers to promote transcription initiation (Jones and Lin, 2017; Konuma et al., 2017; Liu et al., 2013; Shen et al., 2015; Zhang et al., 2016). BRD4 also interacts with the positive transcription elongation factor b (P-TEFb) and facilitates transcription elongation (Jang et al., 2005; Yang et al., 2005). Growing evidence suggests that BRD4 conducts certain functions in DNA replication. BRD4-TICRR interaction is crucial for timely replication initiation (Sansam et al., 2018). TICRR mediates assembly of CMG (CDC45-MCM2-7-GINS) helicase that is required for replication origin firing. Furthermore, BRD4-RFC interaction is required for appropriate S phase progression (Maruyama et al., 2002).

Now that PCNA plays an important role in nascent chromatin assembly, PCNA unloading from nascent DNA should be coordinated with nucleosome deposition. Elg1, a yeast homolog of ATAD5, collaborates with histone chaperone Rtt106 to promote nascent chromatin organization (Gali et al., 2018). However, it is still not elucidated how the activity of ATAD5-RLC is regulated to execute PCNA unloading with nascent chromatin assembly.

Here, we found that BET proteins fine-tune the PCNA unloading activity of ATAD5-RLC. ATAD5 could be divided into the N-terminal domain and the C-terminal domain depending on the function (Figure 3B). The N-terminal domain of ATAD5 directly interacted with the ET domain of BRD4. Especially, chromatin-bound BRD4, which is mediated by acetylated histone, inhibited the PCNA unloading activity of ATAD5-RLC. Deletion or overexpression of BRD4 altered the amount of chromatin-bound PCNA. Our results suggest that PCNA unloading from replicated DNA is regulated by the acetylation status of nascent chromatin.

A

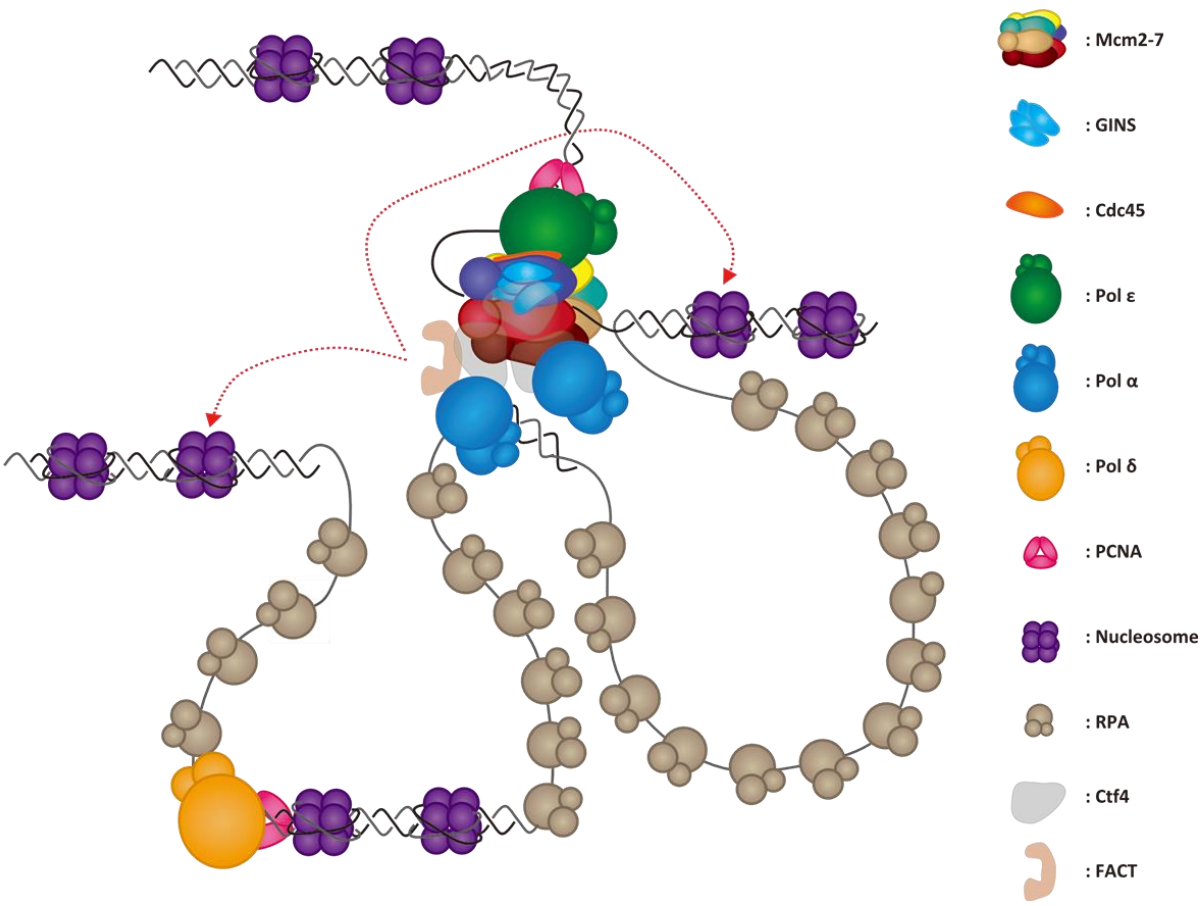

B

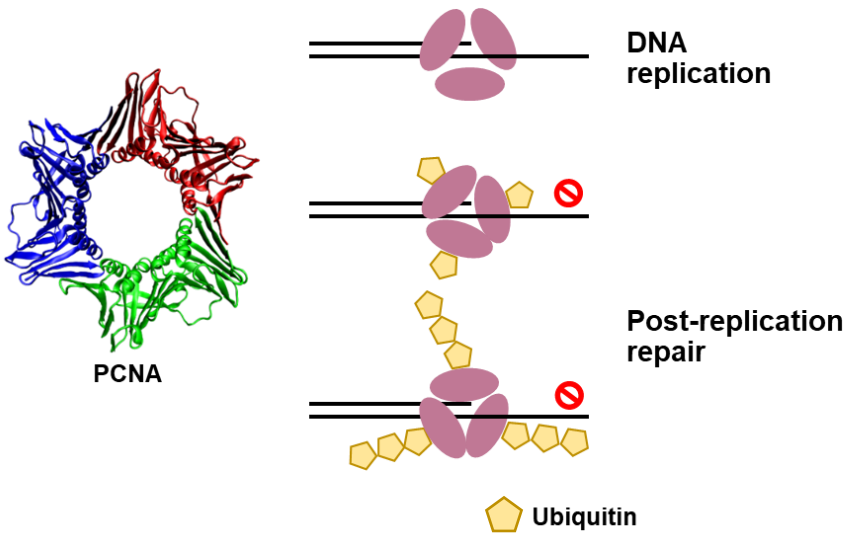

Figure 1. Eukaryotic replication fork structure and the roles of PCNA

(A) Snapshot of eukaryotic replication fork and replication-associated proteins

(B) PCNA functions as a molecular hub for replication and repair proteins. During DNA replication, PCNA interacts with various proteins such as DNA polymerases, Okazaki fragment processing enzymes and histone chaperones to facilitate DNA synthesis. At DNA lesions, PCNA is ubiquitinated for recruitment of translesion polymerase and fork remodeler.

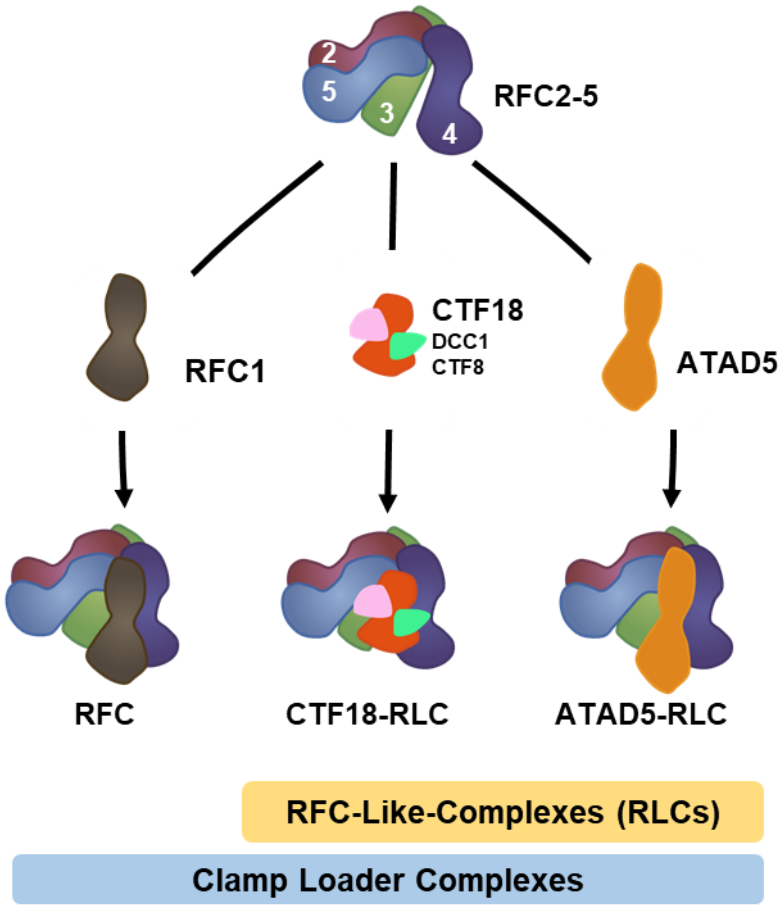

Figure 2. PCNA loading and unloading is mediated by RFC and RFC-like-complexes

DNA association of PCNA is regulated by RFC, CTF18-RLC and ATAD5-RLC. RFC and CTF18-RLC load PCNA to primer-template junction to initiate DNA synthesis. ATAD5-RLC dissociates PCNA from the replicated DNA to complete chromosome duplication.

A

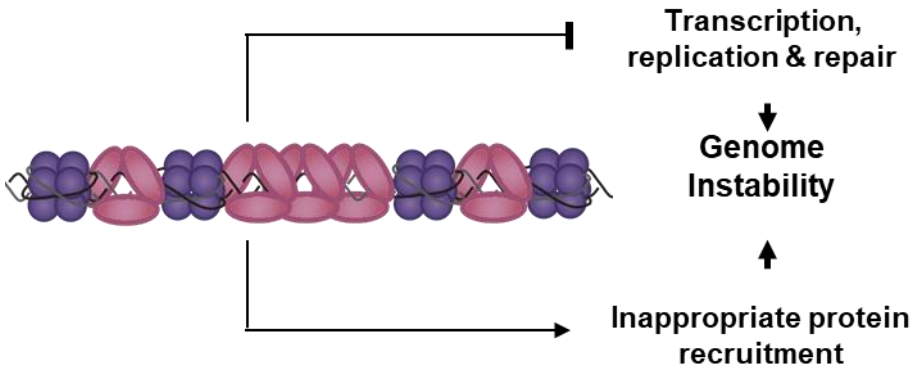

B

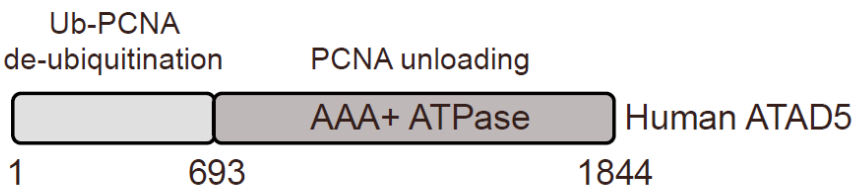

Figure 3. PCNA unloading by ATAD5-RLC is crucial for maintaining genomic integrity

(A) Inappropriate PCNA accumulation on chromatin results in genome instability.

(B) Domains of human ATAD5. The N-terminal domain of ATAD5 is involved in de-ubiquitination of ubiquitinated PCNA. The C-terminal domain of ATAD5 possesses AAA+ ATPase domain and participates in unloading of PNCA from DNA.

2. Materials and Methods

2.1 Cell culture and cell lines

Human HEK293T cell was cultured in Dulbecco's modified Eagle's medium (Hyclone) supplemented with 10% of fetal bovine serum (Hyclone) and 1% of a penicillin-streptomycin solution (GIBCO) at 37◦C and 5% CO_2. HeLa-derived cell lines that stably express FLAG-tagged ATAD5 proteins were generated by means of a Flp-In™ system (Thermo Fisher Scientific). Tetracycline-free serum was used for the maintenance of the stable cell lines carrying a doxycycline-inducible construct. HEK293T and HeLa cells are female.

2.2 Plasmid and siRNA transfection

HEK293T cells were transiently transfected with various plasmids using the X-tremeGENE™ HP DNA Transfection Reagent (Roche). For a protein knockdown, cells were transfected with various siRNAs via Lipofectamine RNAiMAX (Thermo Fisher Scientific). Plasmid- or siRNA-transfected cells were harvested 48 h after transfection for further analysis.

2.3 Plasmids

Wild-type ATAD5 or BRD4 and its mutants were cloned into the p3 x FLAG-CMV10 expression vector (Sigma-Aldrich), pcDNA5/FRT/TO (Thermo Fisher Scientific), or pcDNA3.1 (Invitrogen). All constructs were confirmed by sequencing. Point mutations were introduced by site-directed mutagenesis with the QuikChange Site-Directed Mutagenesis Kit (Agilent Technologies).

2.4 siRNAs

siRNAs specific to the 3' untranslated region (UTR) of ATAD5 mRNA with sequences 5′-GUAUAUUUCUC GAUGUACAUU-3′ (sense) and 5′- UGUACAUCGAGAAAUAUACUU-3′ (antisense) were synthesized by Bioneer (South Korea). Nontargeting control siRNA (AccuTarget Negative Control siRNA) was purchased from Bioneer (South Korea).

2.5 iPOND

iPOND was performed as described by Sirbu et al. (2011) with slight modifications. Briefly, HEK293T cells were pulsed with a medium containing EdU (10 μM, Life Technologies) for 20 min. The EdU-labeled cells were washed once with a medium containing 10 μM thymidine to remove EdU, then a thymidine chase was performed with a medium containing 10 μM thymidine for 0, 10, 30, 60, or 120 min. Cells were cross-linked with1% formaldehyde for 20 min at room temperature, quenched with 0.125 M glycine, and washed with PBS. For the conjugation of EdU with biotin azide,

cells were permeabilized with 0.25% Triton X-100/ PBS and incubated in click reaction buffer (10 mM sodium-L-ascorbate, 20 μM biotin azide (Life Technologies), and 2 mM CuSO4) for 30 min at room temperature. After centrifugation, the pellets were washed once with 0.5% BSA/PBS and twice with PBS. The cells were resuspended in lysis buffer (50 mM Tris-HCl pH 8.0, and 1% of SDS) supplemented with protease inhibitors and were sonicated. The lysates were cleared and then incubated with streptavidin-agarose beads (Novagen) overnight at 4°C. The beads were washed once with lysis buffer, once with 1 M NaCl, and then twice with lysis buffer. To elute proteins bound to nascent DNA, 2 3 SDS Laemmli sample buffer was added to packed beads (1:1; v/v). Samples were incubated at 95°C for 30 min, loaded on a gel for SDS-PAGE, and analyzed by immunoblotting.

2.6 Immunoprecipitation and western blot analysis

Whole-cell lysates were extracted with buffer X (100 mM Tris-HCl pH 8.5, 250 mM NaCl, 1 mM EDTA, 1% of Nonidet P-40, and 5 mM $MgCl_2$) supplemented with the cOmplete protease inhibitor cocktail (Roche), phosphatase inhibitor PhosSTOP (Roche), and 500 U of Benzonase for 40 min at 4°C. Lysates were cleared by centrifugation (13,000 3 g, 4°C, and 5 min). Protein concentration was determined by the Bradford Assay (Bio-Rad). FLAG-tagged ATAD5 proteins were incubated with anti-FLAG M2 agarose affinity beads (Sigma-Aldrich, A2220), and V5-tagged BRD4 proteins were incubated with anti-V5-agarose-affinity beads (Sigma-Aldrich, A7345) for 1 h at 4°C, with constant rotation. The beads were washed three times with buffer X, and the anti-FLAG-bead–bound proteins were eluted with buffer X containing 0.15 mg/ml FLAG peptide. Anti-V5-bead–bound proteins were resuspended in 2 x SDS loading buffer and boiled at 100°C for 5 min. Coimmunoprecipitated proteins were loaded onto SDS-PAGE and analyzed by immunoblotting. The proteins were detected by means of a ChemiDoc MP imaging system (Bio-Rad). The signal intensity of the bands was quantified by ImageLab software version 5.2.1 (Bio-Rad). To detect a phospho-shift, we ran SDS-PAGE in a 5% gel with Phos-Tag™ Acrylamide AAL-107 (25 μM, NARD Institute) and 50 μM $MnCl_2$.

2.7 Antibodies

The following antibodies were used: an anti-FLAG antibody (Sigma-Aldrich, F3165, 1:1000); anti-PCNA (PC10) antibody (Santa Cruz Biotechnology, sc-56, 1:2000); Acetyl-Histone H3 Antibody Sampler Kit (Cell Signaling Technology, #9927, 1:2000); Acetyl-Histone H4 Antibody Set (Merck-Millipore, #17-211, 1:2000); anti–histone H3 antibody (Merck-Millipore, #07-690, 1:5000); anti-BRD2 antibody (Bethyl, A302-583A, 1:1000); anti-BRD3 antibody (Bethyl, A302-368A, 1:1000); anti-BRD4 antibody (Bethyl, A301-985A, 1:1000); Pan-BRD4 antibody (Sigma-Aldrich, AV39076, 1:1000); anti-V5 antibody (Sigma-Aldrich, V8137, 1;2000); anti-UAF1 antibody (Santa Cruz

Biotechnology, sc-514473, 1:500); anti-S tag antibody (Sigma-Aldrich, SAB2702227, 1:5000); anti-phosphohistone H3 (Ser10) antibody (Cell Signaling Technology, #9706, 1:1000); anti-beta-tubulin antibody (Abcam, ab15568, 1:2000); anti-lamin B1 antibody (Abcam, ab16048, 1:1000); anti-phospho-histone H2A.X (Ser139) (Merck-Millipore, #05-636, 1:2000). The anti-human ATAD5 antibody (1:1000) was raised in rabbits.

2.8 AP-MS analysis

For liquid chromatography with tandem mass spectrometry, the gel was destained, and bands were cut out and processed as follows. Briefly, the protein bands were divided into 10 mm sections and subjected to in-gel digestion with trypsin. The tryptic digests were separated by online reversed-phase chromatography on a Thermo Scientific Eazy nano LC 1200 UHPLC system equipped with an autosampler using a reversed-phase peptide trap Acclaim PepMap^{TM} 100 column (75 μm inner diameter, 2 cm length) and a reversed-phase PepMap^{TM} RSLC C18 analytical column (75 μm inner diameter, 15 cm length, 3 μm particle size), both from Thermo Scientific, followed by electrospray ionization at a flow rate of 300 nl/min. The chromatography system was coupled in line with an Orbitrap Fusion Lumos mass spectrometer. Spectra were searched against the UniProt-human DB in Proteome Discoverer 2.1 software via the Sequest-based search algorithm, and comparative analysis of proteins identified in this study was performed in Scaffold 4 Q+S.

2.9 CUPID analysis

Plasmids PKC-δ-mRFP-BRD4B and either mNeongreen-ATAD5 (1–692) WT or BET M2 were cotransfected into HEK293T cells. After 48 h, the cells were treated with a translocation signal activator (PMA) and then fixed with 3.7% formaldehyde. CUPID images were captured by means of a laser scanning confocal microscope (LSM 880, Carl Zeiss) with a C-Apochromat 40X/1.2 water immersion lens (488 nm argon laser/505-550 nm detection range for mNeongreen, 561 nm solid state laser/586-662 nm detection range for mRFP). The fluorescence intensity at a cross-section of the nuclear membrane was analyzed in the ZEN blue software (Carl Zeiss).

2.10 Protein purification

BRD4A was expressed and purified using a Bac-to-Bac Baculovirus expression system (Thermo Fisher Scientific). The expression construct for BRD4A contains an N-terminal 10 x HIS-tag and a C-terminal 3 x FLAG tag. Viruses were prepared in Sf9 cells, and proteins were expressed in Hi-5 cells. ATAD5 (500–800) and BRD4B (444–794) were cloned into bacterial expression vectors pET-19b (Merck-Millipore) and pRSF-1b (Merck-Millipore), respectively, then were expressed in E. coli BL21 (DE3) cells (Enzynomics) and Rosetta 2 (Merck-Millipore). Expression constructs for ATAD5 (500–

800) and its BET M2 mutant contain an N-terminal 10 x HIS-3 x FLAG tag and C-terminal StrepII-HALO tag. BRD4B (444–794) was tagged with an N-terminal 6 x HIS-3 x FLAG-MBP tag and C-terminal S tag. To purify proteins from E. coli cells, 1 L cultures were grown to OD of 0.4, and protein expression was induced by the addition of 1M isopropyl β-$_D$-1-thiogalactopyranoside (IPTG) for 4 h incubation. E. coli cells were resuspended in Buffer H (25 mM HEPES pH 7.5, 1 mM EDTA, 1 mM EGTA, 2.5 mM magnesium acetate, 10% of glycerol, 1 mM ATP, and 0.02% of NP40) plus 300 mM KCl, with a complete protease inhibitor cocktail (Roche) and were lysed with lysozyme. The cell lysates were cleared by ultracentrifugation (36,000 x g, 60 min). Proteins were purified by sequential application of cOmplete HIS-Tag resin (Roche), anti-FLAG M2 agarose resin (Sigma-Aldrich), and ion exchange chromatography. Purified proteins were analyzed by SDS-PAGE.

2.11 An in vitro pull-down assay

10 pmol of purified wild-type or BET M2 FLAG-ATAD5 (500–800)-StrepII-HALO and 10 pmol of purified MBP-BRD4B (444–794)-S were mixed in Buffer H plus 100 mM KCl for 1 h at 4°C. The mixtures were combined with Streptactin Sepharose beads (GE Healthcare) for 1 h at 4°C. Beads were collected and washed three times with Buffer H plus 100 mM KCl. Bead-associated proteins were eluted with Buffer H plus 100 mM KCl containing 10 mM desthiobiotin, then analyzed by immunoblot or Krypton staining.

2.12 Chromatin fractionation

This procedure was performed as described previously (Kang et al., 2019). Cells were lysed with buffer A (100 mM NaCl, 300 mM sucrose, 3 mM $MgCl_2$, 10 mM PIPES pH 6.8, 1 mM EGTA, and 0.2% of Triton X-100, containing the phosphatase inhibitor PhosSTOP (Roche) and cOmplete protease inhibitor cocktail (Roche) for 8 min on ice. Crude lysates were centrifuged at 5000 x g at 4°C for 5 min to separate the chromatin-containing pellet from the soluble fraction. The pellet was digested with 50 U of Benzonase (Enzynomics) for 40 min in RIPA buffer (50 mM Tris-HCl pH 8.0, 150 mM NaCl, 5 mM EDTA, 1% of Triton X-100, 0.1% of SDS, 0.5% of sodium deoxycholate, 1 mM PMSF, 5 mM MgCl2, containing the phosphatase inhibitor PhosSTOP (Roche) and cOmplete protease inhibitor cocktail (Roche) to extract chromatin-bound proteins. The chromatin-containing fractions were clarified by centrifugation (13,000 x g, 4°C) for 5 min to remove debris. Protein concentration was determined by the Bradford Assay (Bio-Rad), and the proteins were analyzed by western blotting.

2.13 An EU incorporation assay

HeLa cells harboring doxycycline-inducible wild-type or BET M2 ATAD5 were labeled with 10 μM EU for 30 min. For confocal microscopy analysis, samples were prepared using the Click-iT™ RNA Alexa Fluor™ 594 imaging Kit (Invitrogen) and subjected to confocal microscopy analysis (LSM 880, Carl Zeiss). The fluorescence intensity was analyzed in the ZEN blue software (Carl Zeiss).

2.14 QUANTIFICATION AND STATISTICAL ANALYSIS

Quantification of immunoblots was performed using Bio-Rad Image Lab. Statistical analyses were completed using GraphPad Prism. Statistical details of individual experiments are described in the figure legends and results section. Unless otherwise stated, all experiments were performed three times and representative experiments were shown. Bar graphs with mean and standard deviation were presented. Individual data points were overlaid with graphs as scatter dot plot. In all cases, *$p < 0.05$, **$p \leq 0.01$, ***$p \leq 0.001$, and ****$p \leq 0.0001$.

3. Results

3.1 ATAD5 is enriched on nascent DNA and BET proteins interact with ATAD5

The PCNA unloading is thought to be mediated by C-terminal ATAD5 (693-1,844) which contains ATPase domain and binding domain of RFC2-5. As expected from its role in replication, ATAD5 is enriched on nascent DNA. Of note, iPOND analysis revealed that ATAD5 (1-692) was strongly enriched on nascent DNA and dissociated from nascent DNA after thymidine chase procedure, when PCNA disappeared from the nascent DNA (Figure 4A). The coexistence of PCNA and ATAD5 (1-692) implies that the unloading activity of ATAD5-RLC could be regulated by its N-terminal domain.

Not only ATAD5 (1-692) binds to UAF1, but also it contains several well-conserved motifs whose function has not been characterized. Interacting proteins that binds to these motifs may act a regulatory factors that control ATAD5-RLC activity. To uncover the functional regulators of ATAD5-RLC, Mi-Sun Kang affinity purified proteins interacting with ATAD5 (1-692) after transient expression. Mass spectrometric analysis was performed for the identification of the co-isolated proteins (Figure 4B). Interestingly, BET proteins –BRD2, BRD3 and BRD4 – were found to be co-isolated with ATAD5 (1-692). It has been reported that BET proteins interact with acetyl histones and our iPOND analysis showed that H4K5Ac and H4K12Ac are enriched on nascent DNA (Figure 4A).

A

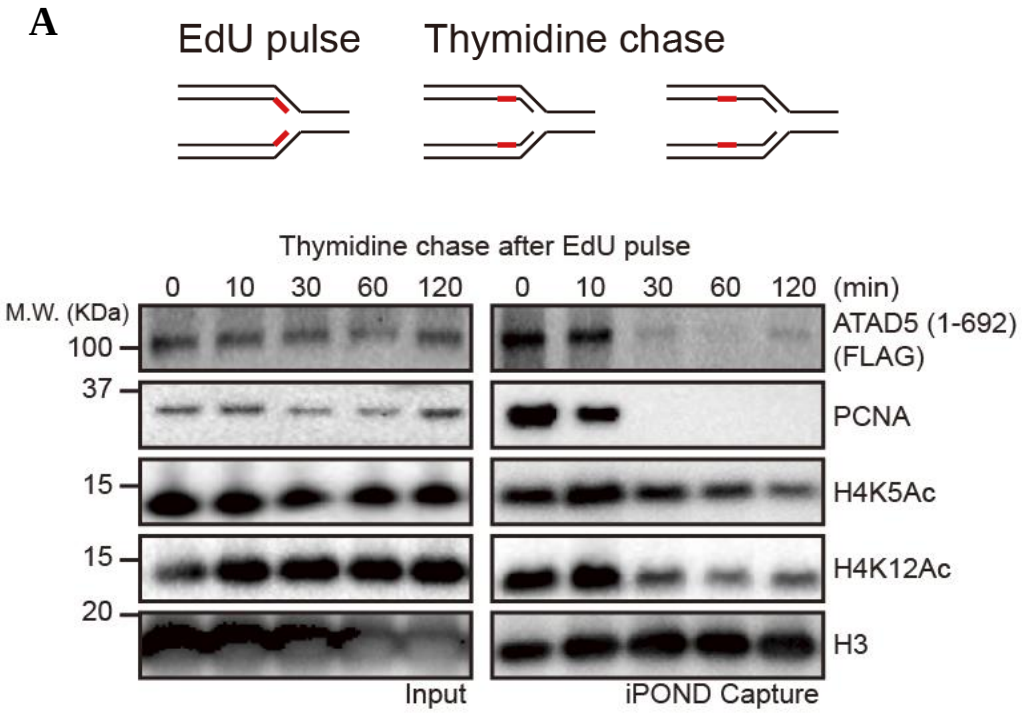

B

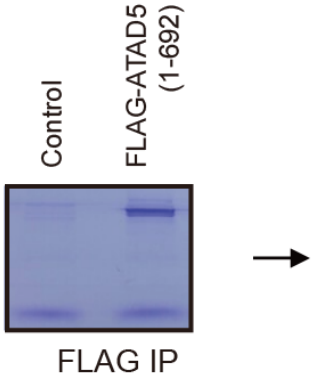

Identified proteins	Peptide numbers	
	Control	ATAD5 (1-692)
ATAD5	4	68
UAF1	0	33
BRD2	0	12
BRD3	0	2
BRD4	0	12

Mass Spec analysis after FLAG IP

Figure 4. ATAD5 is enriched on nascent DNA and BET proteins interact with the N-terminal domain of ATAD5

(A) N-terminal domain of ATAD5 binds to nascent DNA.
Top panel: Schematic diagram of iPOND (isolation of proteins on nascent DNA) after EdU pulse-chase. Bottom panel: The enriched proteins on nascent DNA was analyzed by immunoblotting after iPOND. N-terminal domain of ATAD5 – ATAD5 (N693) – and PCNA are enriched on nascent DNA and then gradually released from nascent DNA as replication fork proceeds. Acetylation on Lysine 5 and 13 of histone H3 were also enriched on nascent DNA.
(*iPOND was conducted by Sunyoung Hwang and Mi-Sun Kang Ph.D.*)

(B) BET family proteins interact with ATAD5 (1-692). Affinity purification mass spectrometry (AP-MS) was carried out with FLAG-ATAD5 (1-692). Analysis of co-purified proteins with FLAG-ATAD5 (1-692) showed that BRD2, BRD3 and BRD4 bound to N-terminal domain of ATAD5.
(*AP-MS was conducted by Mi-Sun Kang Ph.D, Byung-Gyu Kim Ph.D and Na Young Ha.)*

3.2 The ET domain of BET proteins interacts with ATAD5

For further investigation about the ATAD5-BRD4 interaction, a series of BRD4 deletion mutants were prepared. Immunoprecipitation with C-terminal deletion mutants of BRD4 revealed that the ET domain of BRD4 was important for ATAD5 binding (Figure 5A). An ET domain-null BRD4 (1-597) could not interact with ATAD5. Then, I tested whether the region upstream of the BRD4 ET domain is essential for ATAD5 binding. Immunoprecipitation results showed that the ET domain alone could bind to ATAD5 (Figure 5B). Moreover, region upstream of the ET domain enhanced the interaction between ATAD5 and BRD4. Overall, these results suggested that BRD4 interacts with ATAD5 through its ET domain.

A

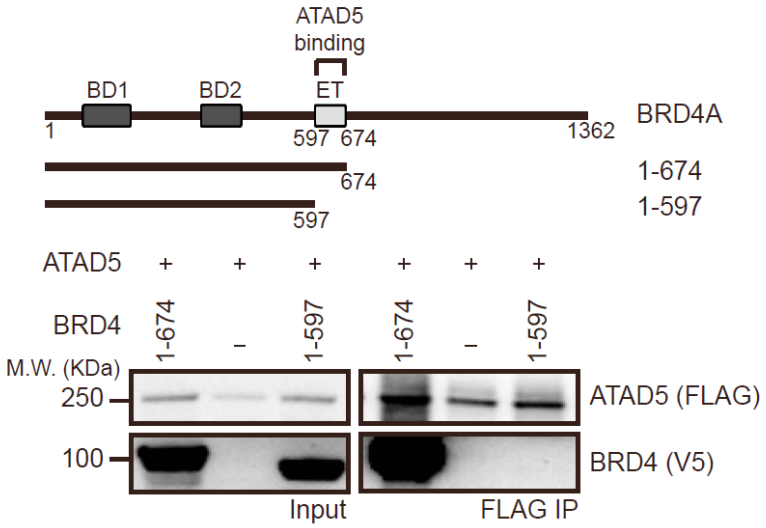

B

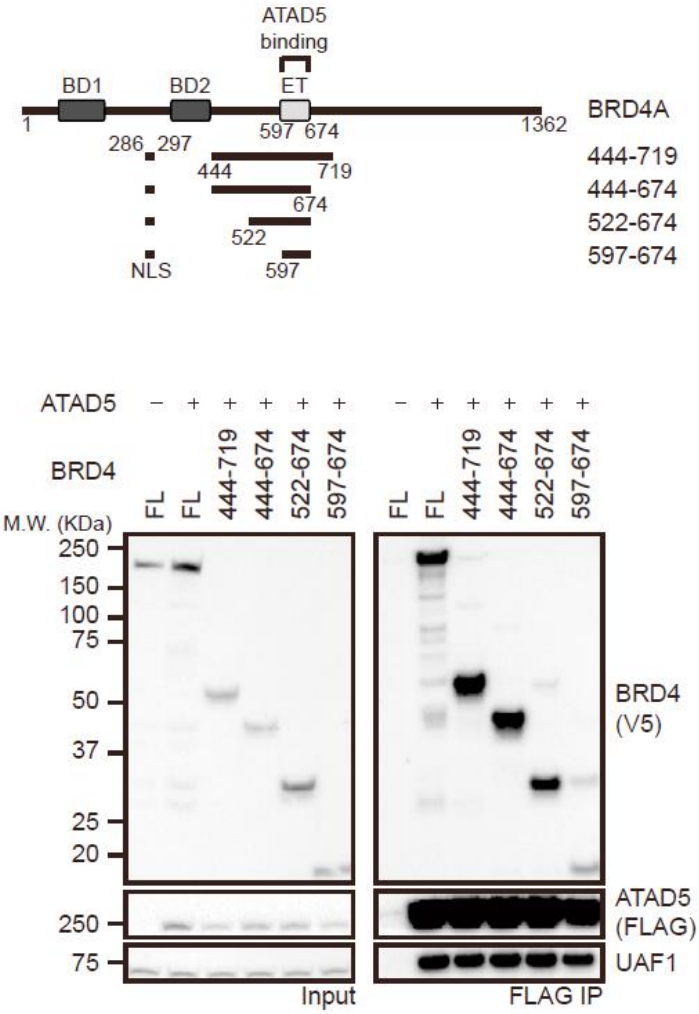

Figure 5. The ET domain of BET proteins is crucial for the interaction with ATAD5

(A) The ET domain-null BRD4 did not interact with ATAD5. Top: a diagram of wild type and truncated forms of BRD4. Bottom: FLAG-immunoprecipitation was performed to examine the interaction between ATAD5 and BRD4 mutants. Deletion of BRD4 (597-674), ET domain of BRD4, abrogated the interaction between BRD4 and ATAD5.
(Immunoprecipitation was conducted by Mi-Sun Kang Ph.D.)

(B) The ET domain of BRD4 is an ATAD5-binding motif. Top: a diagram of wild type and truncated forms of BRD4 used in the experiments. Nuclear localization sequence (NLS) were fused to all N-terminal deletion mutants. Bottom: Immunoprecipitation experiments revealed that BRD4 (597-674) was sufficient for ATAD5 binding.

3.3 ATAD5 (596-692) is an ET domain-binding motif.

ATAD5 (596-692) sequences are well conserved among various species (Figure 6A) and predicted to form a β-stranded structure by a secondary-structure prediction program. Of note, polypeptide sequences around $R^{656}MK^{658}$ of ATAD5 are similar to BRD4-binding motifs of the MLV integrase, NSD3, and CHD4 (Crowe et al., 2016; Zhang et al., 2016). Based on these conserved sequences, two ATAD5 mutants, which were designated as BET M1 ($E^{643}LI^{656}$ to AAA) and BET M2 ($R^{656}MK^{658}$ to AAA), were prepared. Wild-type and mutant FLAG-ATAD5 were transiently expressed. Immunoprecipitation of ATAD5 showed that BET M2 mutant failed to interact with endogenous BRD4A (Figure 6B). These results indicate that well conserved β-stranded structure of ATAD5 is crucial for BET protein binding.

BRD4-binding motifs contain I/L-R/K-f-R/K-f (f: any hydrophobic amino acid). Some studies showed that two negatively charged amino acid residues in the BRD4 ET domain, E653 and D655, are crucial for the binding to the MLV integrase (Crowe et al., 2016). So, these two residues were mutated into alanine (hereafter referred to as EDAA) or positively charged amino acids (hereafter referred to as EDRK), then I examined whether these mutations affect ATAD5 binding (Figure 6C). As expected, mutation of EDAA and EDRK significantly disrupted the interaction between ATAD5 (1-692) and BRD4 (1-719). Full-length BRD4 (EDAA) also failed to interact with endogenous ATAD5 (Figure 6C right). However, reduced ATAD5 binding caused by the EDRK mutation in the BRD4 ET domain was not restored by a charge conversion mutation in the ATAD5 BET BD (ATAD5 R656E K658D) (Figure 6D). This finding suggested that the BRD4-ATAD5 interaction does not represent simple electrostatic interactions between charged amino acids.

A

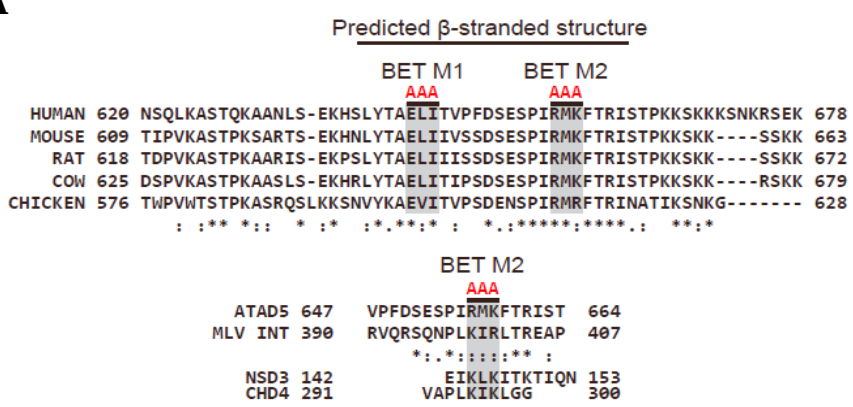

B

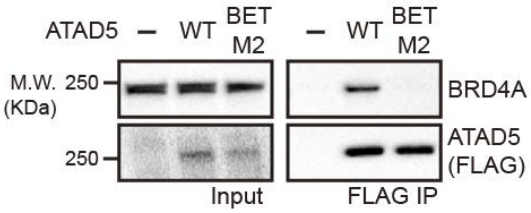

C

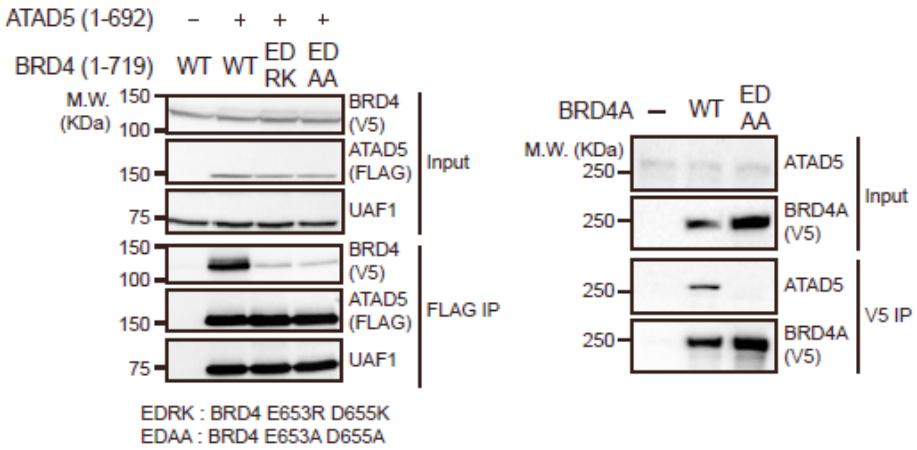

D

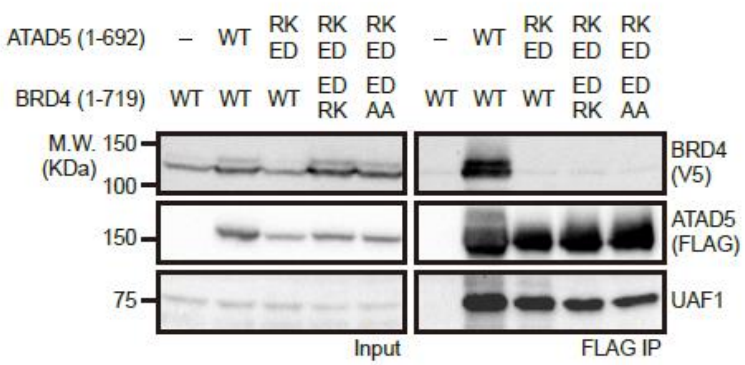

Figure 6. Conserved β-stranded structure of ATAD5 is a BRD4 ET domain-binding motif

(A) ATAD5 (643-658) is well conserved among various species and predicted to form β-strand structure. BET M1 and BET M2 respectively represent the mutations of ATAD5 (E643LI645 to AAA) and ATAD5 (R656MK658 to AAA). The sequences of ATAD5 R656MK658 share similar properties with the BRD4-binding motif of MLV integrase, NSD3 and CHD4.

(B) ATAD5 BET M2 mutants cannot bind to BRD4. FLAG-ATAD5 and its mutant were transiently expressed and FLAG immunoprecipitation was performed. ATAD5 BET M2 diminished the binding to endogenous BRD4.

(C) Negatively charged residues in BRD4 ET domain are crucial for ATAD5 binding. Two negatively charged amino acids in BRD4 ET domain were mutated to positively charged amino acids (EDRK) or to alanine (EDAA). Left: Fragments of ATAD5 (1-692) and BRD4 (1-719) were transiently expressed and FLAG immunoprecipitation was performed. Both negative charge-null BRD4 mutants failed to interact with ATAD5. Right: Endogenous ATAD5 were co-immunoprecipitated with transiently expressed BRD4. EDAA mutants of BRD4 failed to interact with ATAD5.

(D) Electrostatic interaction is not sufficient for BRD4-ATAD5 interaction. The positively charged amino acid residues of ATAD5 R656 and K658 were mutated to negatively charged glutamate and aspartate, respectively – ATAD5 (RKED). FLAG-immunoprecipitation revealed that ATAD5 (RKED) mutation did not restore the interaction with BRD4 (EDRK).

3.4 ATAD5 directly interacts with BRD4 through its ET domain-binding motif

To test the intracellular interaction between BRD4 and ATAD5, cell-based unidentified protein interaction discovery (CUPID) analysis (Lee et al., 2011) was introduced. The CUPID analysis has been used for real-time monitoring of protein–protein interactions. In CUPID, a bait protein is fused to protein kinase C-δ (PKC-δ) that migrates to the cell membrane during treatment with phorbol-12-myristate 13-acetate (PMA). A bait-binding protein comigrated with the bait-PKC-δ fusion to the cell membrane. I performed CUPID analysis with mNeongreen-ATAD5 (1–692) and PKC-δ-mRFP-BRD4B (Figure 7A). Both proteins dispersed throughout the nucleus before PMA treatment. Upon PMA treatment, ATAD5 (1–692) comigrated with PKC-δ-BRD4B to the nuclear membrane. By contrast, BET M2 ATAD5 (1–692) did not comigrate with PKC-δ-BRD4B.

To determine whether BRD4 directly interacts with ATAD5, I conducted an in vitro pull-down experiment with purified proteins. I purified the BET BD-containing region of ATAD5, ATAD5 (500–800), using a bacterial expression system (Figure 7B). I also purified full-length BET proteins using insect cell expression system. Purified proteins were mixed, and then StrepII-tagged ATAD5 (500–800) was isolated using streptactin sepharose beads. All BET proteins was found to be co-isolated with ATAD5 (500-800) (Figure 7C). Next, I performed in vitro pull-down assay with wild-type or BET M2 ATAD5 (500-800) and BRD4B (444-794) (Figure 7D). To increase stability and solubility, an MBP and a HALO tag were fused to BRD4B (444–794) and ATAD5 (500–800), respectively. BRD4B (444–794) was coisolated with ATAD5 (500–800). Nonetheless, mutation BET M2 in the BET BD of ATAD5 abrogated the coisolation. These data clearly showed that the BET BD of ATAD5 directly binds to the ET domain of BRD4.

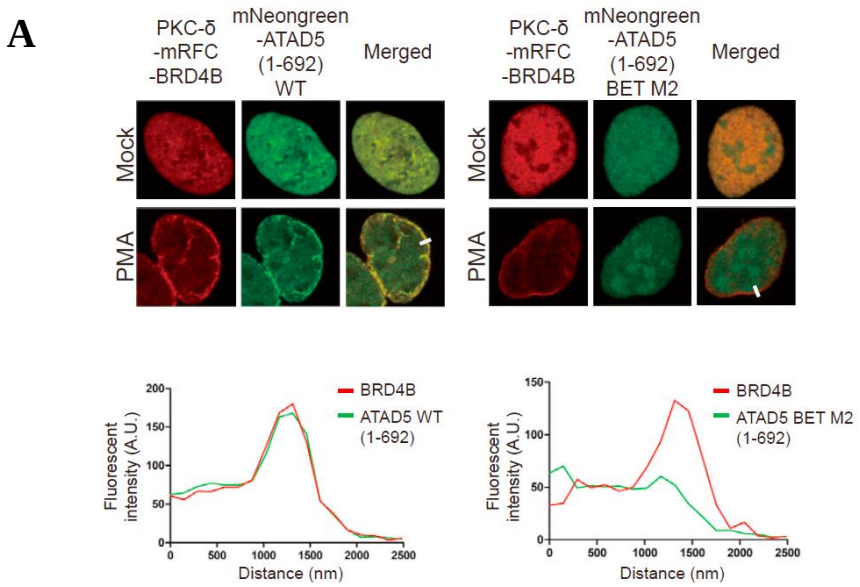

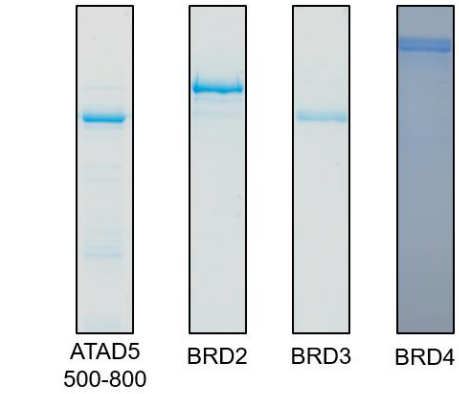

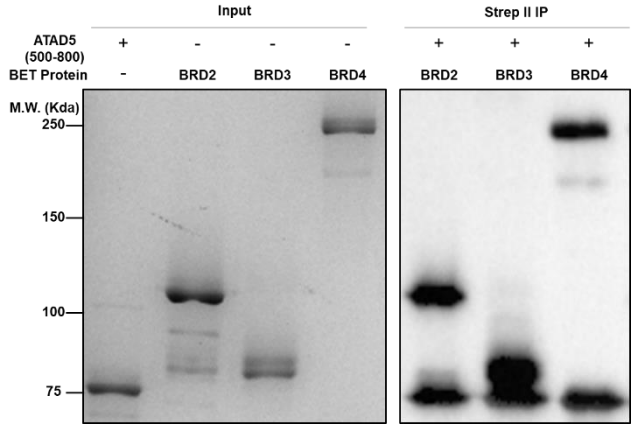

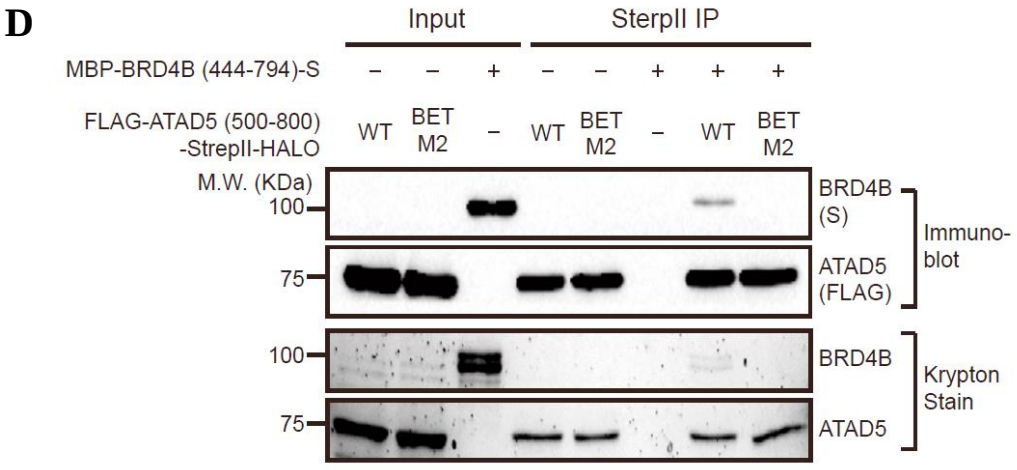

Figure 7. ATAD5 directly interacts with BRD4 through its ET domain-binding motif

(A) CUPID assay was performed to examine the interaction between ATAD5 and BRD4 in cellular level under confocal microscopy. Addition of PMA induced the translocation of PKC-δ-mRFP tagged BRD4 to nuclear membrane. Wild type of mNeongreen ATAD5 (1-692) was comigrated with BRD4 to the nuclear membrane, but the BET M2 mutant did not. White bars indicate the cross-section used for quantification.

(B) BET binding domain of ATAD5 and BET proteins were purified for in vitro pull down assay. FLAG-ATAD5 (500-800)-StrepII-HALO and HIS-BRD2, 3 and 4-FLAG were prepared.

(C) ATAD5 (500-800) directly interacts with BET proteins. In vitro pull-down assay was performed with indicated proteins. BRD2, BRD3 and BRD4 were co-immunoprecipitated with Strep II tagged ATAD5.

(D) ATAD5 (500-800) directly interacts with BRD4 through ET domain-binding motif. BRD4 co-purified with wild-type ATAD5 but not with ATAD5 BET M2 mutant.

3.5 BRD4 binding to ATAD5 does not interfere with mRNA transcription

As previously reported, BRD4 is a key transcription regulator for many genes. BRD4 recruits transcriptional regulators to chromatin and interacts with chromatin remodelers to facilitate transcription initiation. I tested whether the binding of ATAD5 to BRD4 affects transcription. Endogenous ATAD5 was depleted by small interfering RNA (siRNA) transfection, and doxycycline was applied to turn on wild type of full length ATAD5 and BET M2 ATAD5. Global transcription of each sample was detected by a 5-ethynyl-uridine (EU) incorporation (Figure 8A). EU-labeled RNA was detected by Alexa-594 azide using confocal microscopy. Overexpressed ATAD5 did not affect the mean intensity of EU signal in both case of wild type and BET M2. Interestingly, ATAD5-depleted cells showed decreased incorporation of EU (Figure 8B). However, the add-back of exogenous ATAD5 into ATAD5-depleted cells restored EU signals in both case of wild type and BET M2 mutant. These results suggested that ATAD5 function is required for efficient cellular transcription, but BRD4-ATAD5 interaction is not essential for ATAD5 dependent transcriptional regulation.

A

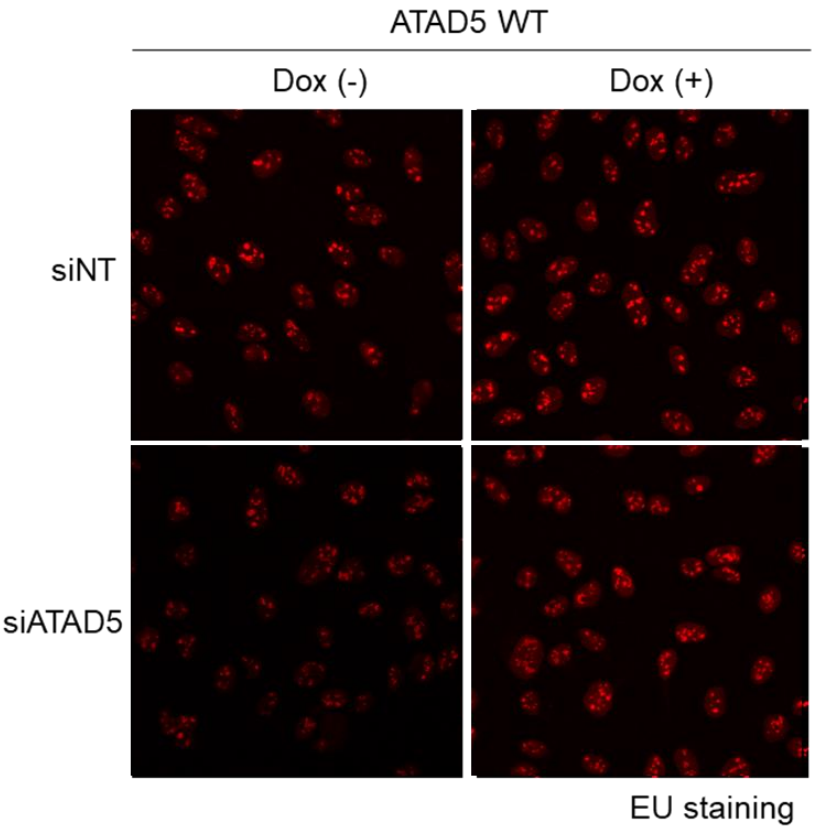

B

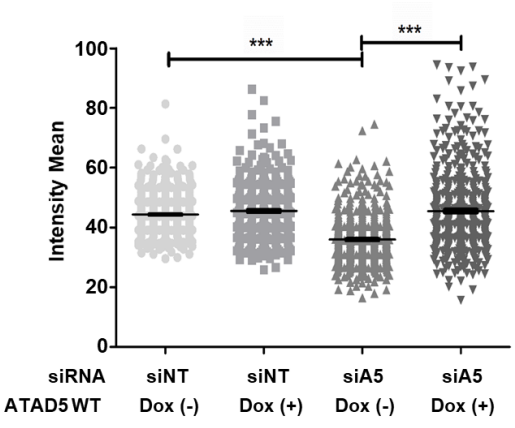

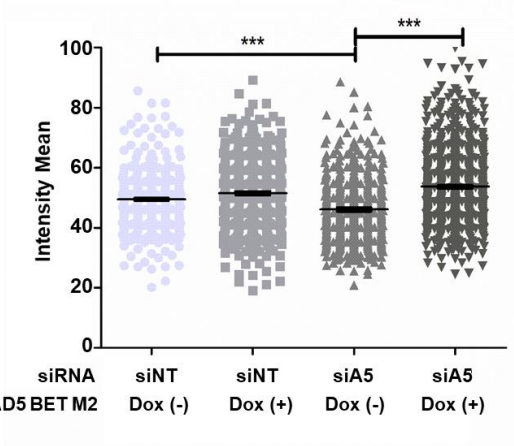

Figure 8. BRD4 binding to ATAD5 does not interfere with global mRNA transcription

(A) Representative image of EU staining. Endogenous ATAD5 was depleted by siRNA and wild-type and BET M2 ATAD5 were expressed from the genome-integrated doxycycline-inducible cassette. Transcribing mRNA incorporated EU was detected by Alexa-594 azide. EU density of each sample was analyzed by confocal microscopy.

(B) Quantification of incorporated EU intensity from data in (A). ATAD5-deficient cells show decreased EU intensity. Add-back of exogenous wild-type or BET-binding defective ATAD5 restored EU signal. A relative mean intensity of each cell was quantified from the data ($n = 300\sim500$, $***p \leq 0.001$). The error bar indicates SD.

3.6 Inhibition of BRD4-acetylated histone binding decreases the amount of chromatin bound PCNA

Acetyl-histones such as H4K5Ac and H4K12Ac are enriched in nascent chromatin and bromodomain (BD) of BET proteins bind to these histone marks. Given that ATAD5 plays a role in nascent DNA, it is possible that ATAD5, BRD4 and acetyl-histones cooperate to properly unload PCNA from nascent chromatin. Therefore, we examined whether acetyl histone-bound BRD4 regulates PCNA unloading of ATAD5. JQ1 is an inhibitor for BET proteins that interferes with the interaction between BRD4 and acetyl-histones (Filippakopoulos et al., 2010). After JQ1 treatment, amounts of nascent DNA–bound ATAD5, BRD4A, and PCNA were examined by iPOND analysis (Figure 9). Treatment with JQ1 significantly reduced the amount of nascent DNA-bound BRD4A. Of note, the PCNA quantity on nascent DNA was diminished by the application of JQ1 without affecting the amount of chromatin-bound ATAD5. These results suggested that BRD4 negatively regulates PCNA unloading on the nascent chromatin.

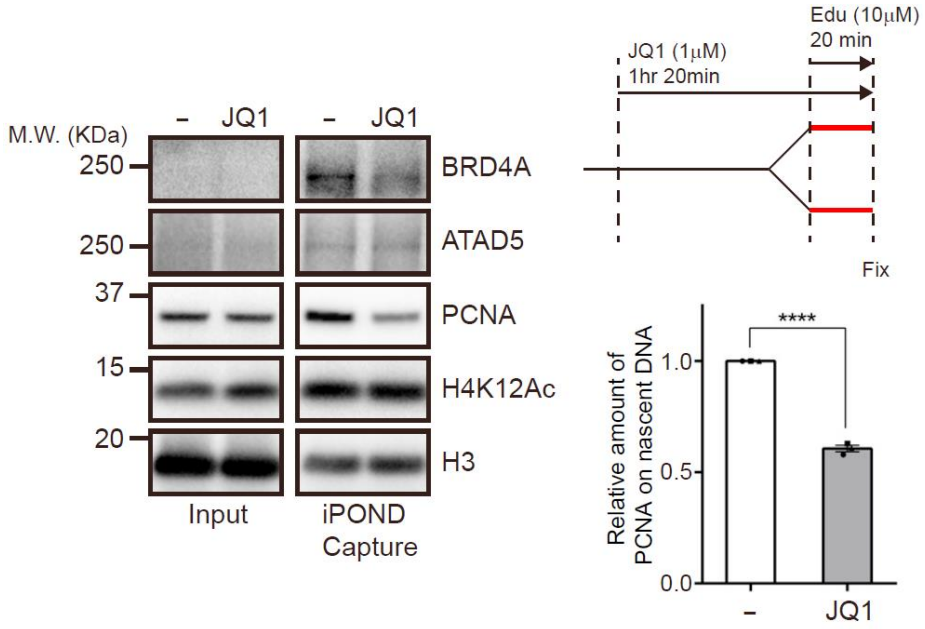

Figure 9. Inhibition of BRD4-acetylated histone binding decreases the amount of nascent chromatin bound PCNA

JQ1 treatment significantly reduces the retention of PCNA on the nascent chromatin. iPOND analysis was performed to examine the nascent DNA-bound proteins under 1 μM JQ1 treatment. The quantity of ATAD5 bound to nascent chromatin was not affected by JQ1. JQ1 reduces the nascent DNA association of BRD4 and PCNA. A relative PCNA amount on nascent DNA was quantified from the data (n = 3, ****$p \leq 0.0001$). The error bar indicates SD.
(*iPOND was conducted by Sunyoung Hwang and Mi-Sun Kang Ph.D.*)

3.7 The level of chromatin bound PCNA is regulated by ATAD5-BRD4 interaction

If BRD4 inhibits PCNA unloading from nascent chromatin, then BRD4 overexpression should result in the accumulation of PCNA in chromatin. I examined the effect of BRD4A overexpression on PCNA unloading (Figure 10A and 10B). The overexpression of BRD4A increased the amount of chromatin-bound PCNA. In contrast, an ET domain mutant of BRD4A—BRD4A (EDAA)—did not induce the accumulation of PCNA in chromatin. These results also support the notion that BRD4 inhibits PCNA unloading through its interaction with ATAD5.

As previously reported, the add-back of exogenous ATAD5 into ATAD5-depleted cells reduced the chromatin-bound PCNA amount (Figures 10C and 10D). ATAD5 (E1173K, EK) is an ATPase motif mutant and is deficient in PCNA unloading (Kang et al., 2019). Accordingly, the expression of ATAD5 (E1173K) in ATAD5-depleted cells failed to decrease the chromatin-accumulated PCNA amount. Interestingly, the add-back of ATAD5 (BET M2) more strongly diminished the chromatin-accumulated PCNA amount as compared to the wild-type add-back group. This result also supports the notion that BRD4A binds to ATAD5 and inhibits the PCNA-unloading activity of ATAD5-RLC.

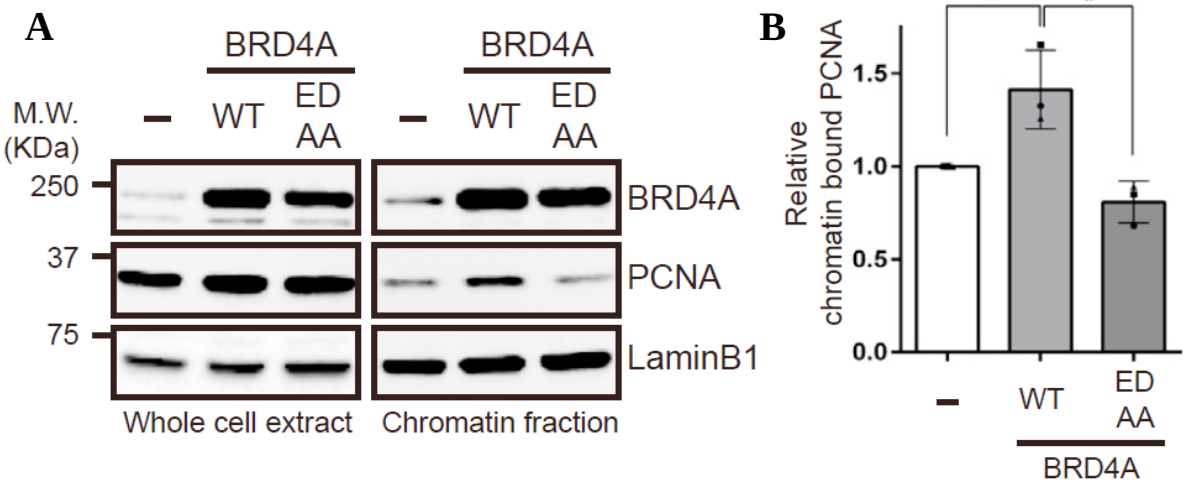

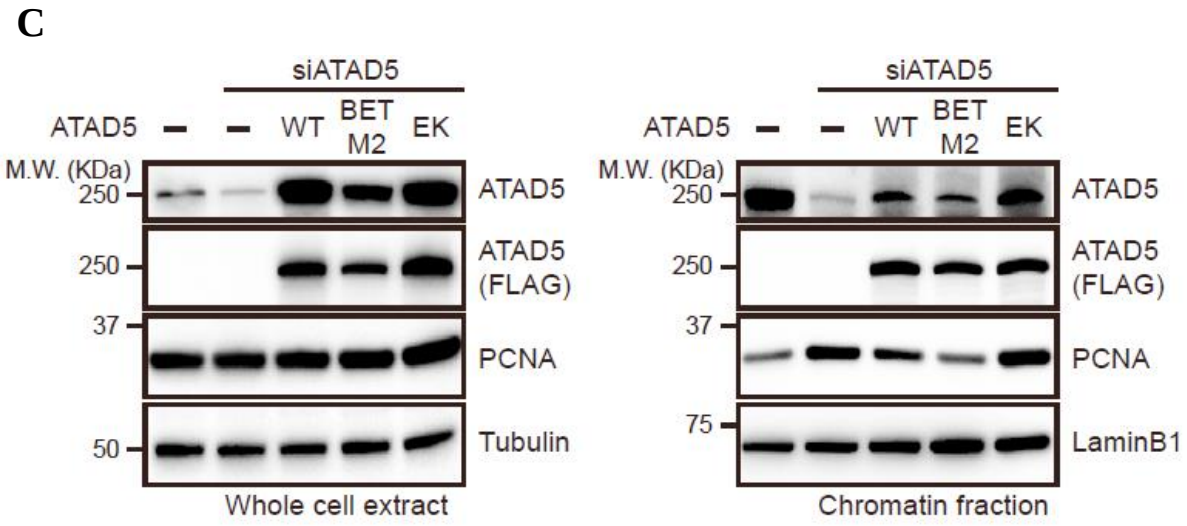

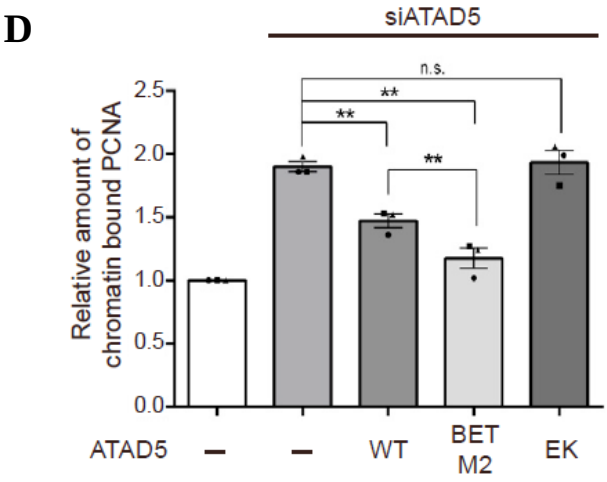

Figure 10. The level of chromatin bound PCNA is regulated by ATAD5-BRD4 interaction

(A) Overexpression of BRD4 inhibits PCNA unloading. Wild type or ATAD5-binding-defective BRD4A were transiently expressed and chromatin-bound PCNA was analyzed by chromatin fractionation. Wild-type of BRD4 induced the accumulation of PCNA on chromatin, but BRD4 (EDAA) did not.

(B) Quantification of (A). A relative PCNA amount on chromatin was quantified from the data ($n = 3$, $*p < 0.05$). The error bar indicates SD.

(C) BET M2 mutant ATAD5 more robustly unloads PCNA as compared to the wild type. Wild-type, BET M2, or E1173K mutant ATAD5 was transiently expressed in endogenous ATAD5-depleted cells. After chromatin fractionation, chromatin-bound PCNA was analyzed by immunoblotting. Blots of a whole-cell extract are presented as a control. Less PCNA was observed on the chromatin of BET M2 mutant-expressing cells compared to the wild-type group.

(D) A relative PCNA amount on chromatin was quantified from the data in (C) ($n = 3$, $**p \leq 0.01$). The error bar indicates SD.

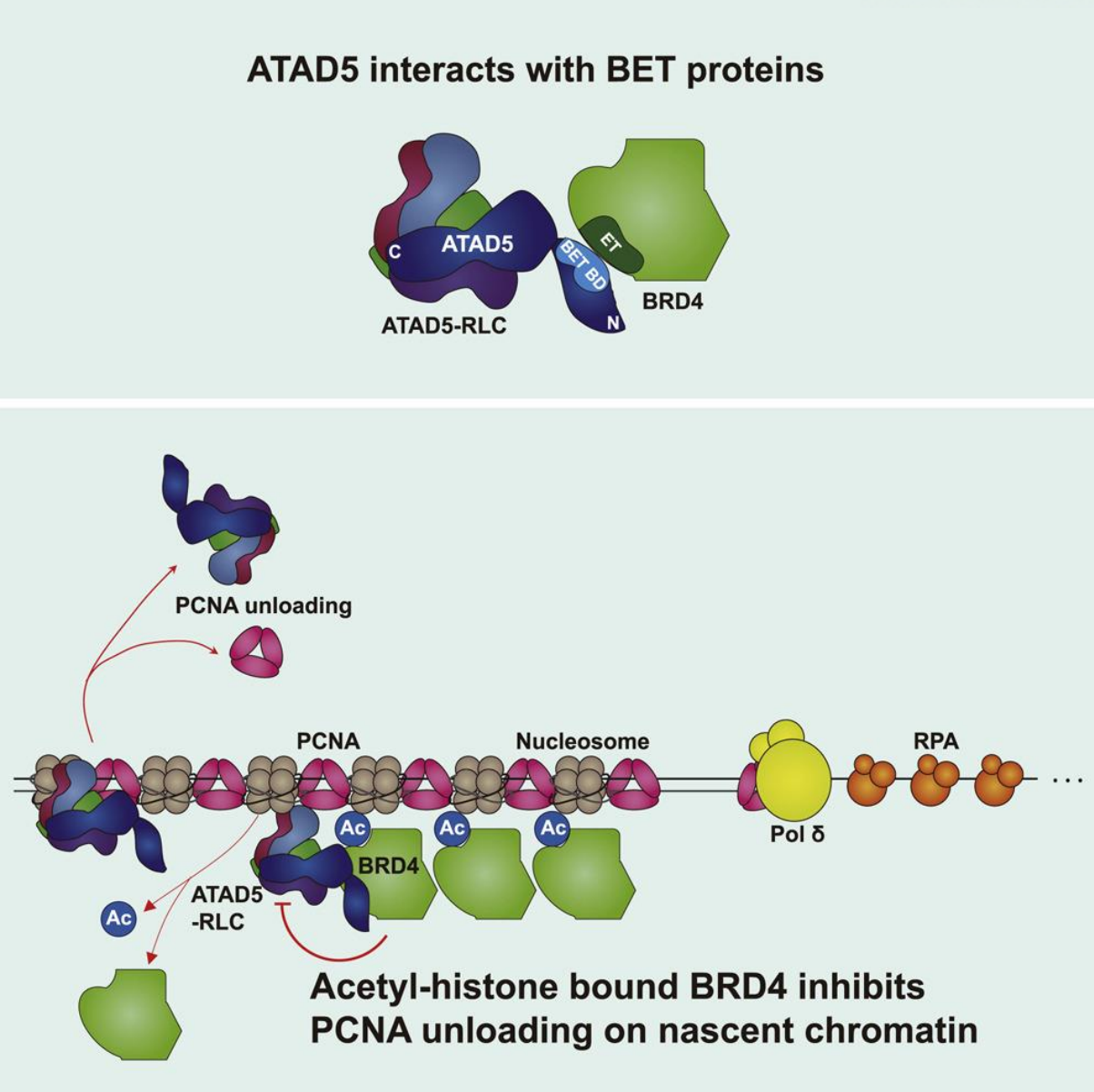

Figure 11. BRD4 fine-tunes the PCNA unloading activity of ATAD5-RLC

β-stranded structure of ATAD5 BET BD directly binds to ET domain of BRD4. Acetylated histone bound BRD4 finely regulate PCNA unloading activity of ATAD5-RLC on nascent chromatin.

4. Discussion

Epigenetic status has been reported to get involved in DNA replication. TICRR binds to BET proteins on euchromatin to regulate the spatiotemporal replication initiation (Sansam et al., 2018). The bromo adjacent homology (BAH) domain of origin recognition complex 1 (ORC1) recognizes methylated histone to enhance chromatin loading of ORC (Kuo et al., 2012). In addition, nucleosome landscape modulates the origin licensing and helicase activation in vitro (Azmi et al., 2017). Here, we found that chromatin status also regulates the PCNA unloading which is the later step of replication (Figure 11).

Given that the synthesis of a large number of Okazaki fragments is simultaneously done during S phase, efficient usage of PCNA is essential in order to complete genome duplication. For discontinuous lagging-strand synthesis, PCNA should be constantly loaded onto DNA. In the same manner, accumulated PCNA must be removed from the nascent DNA for efficient DNA replication. PCNA participates in nucleosome deposition on the replicated DNA, but abnormal PCNA retention on DNA could interfere with chromatin organization. Therefore, fine-regulation of PCNA cycling is required for not only Okazaki fragment synthesis, but also proper post-replicative chromatin assembly. Here, we found that acetyl-histone associated BRD4 negatively regulate PCNA unloading of ATAD5-RLC (Figure 9 and 10). BRD4 may function as a 'safety break' that keeps ATAD5-RLC inactive until PCNA conducts its role on nascent DNA. The conserved β-stranded structure is positioned immediately upstream of the PCNA-unloading domain of ATAD5. To open and unload a PCNA ring, the pentameric surface of ATAD5-RLC binds to the front face of a PCNA homotrimer. The interaction between acetyl-histone-bound BRD4 and ATAD5 may interfere with the access of ATAD5-RLC to PCNA.

BRD4 binds to ATAD5 through its ET-domain (Figure 5). As a key transcription factor as well as chromatin reader, a lot of researches have been focused on bromodomain (BD) and carboxyl-terminal domain (CTD) of BRD4. Recently, ET-domain of BRD4 is emerging as a regulatory region involved both in transcription and replication. BRD4 interacts with histone modifiers including NSD3 and JMJD6 to regulate transcription (Shaila et al., 2011). In addition, DNA replication initiation is regulated through BRD4-TICRR interaction, which is mediated by ET domain of BRD4 (Sansam et al., 2018). As a highly conserved domain throughout BET proteins, ET domain may act as versatile cellular function by mediating protein interaction. Also, BRD4 is regarded as a major therapeutic target in many diseases because of its pivotal roles in cell proliferation (Korb et al., 2017; Sun et al., 2018; White et al., 2019). Considering a series of studies that BRD4 is involved in replication, the effect of inhibiting BRD4 should be considered for replication as well.

Because BRD4 is closely involved in transcription, we examined the possibility that BRD4-ATAD5 interaction is related to transcription (Figure 8). However, abrogation of BRD4-ATAD5 interaction did not reduce the EU incorporation into transcribing mRNA. Of note, the depletion of ATAD5 significantly reduced the incorporation of EU and add-back of exogenous ATAD5 restored EU signal. It suggests that ATAD5 may play a certain role in transcription. Involvement of ATAD5 in transcription has not been fully elucidated. It has been reported that ATAD5 interacts with various kinds of proteins involved in transcription. In yeast, Elg1 interacts with Rtt106, a histone chaperone that is implicated in regulation of transcription (Gali et al., 2018). In drosophila, Elg1 complex interacts with the Enok acetyltransferase complex which plays a positive role in transcriptional activation (Fu et al., 2016). A study about transcription-related function of ATAD5 could provide a novel insight how a replication factor regulates transcription.

Newly synthesized histones that are deposited on nascent DNA have acetylation on Lysine 4 and Lysine 12 of histone H4 in mammalian cells. It has been suggested that these acetylation marks promote nucleosome deposition on nascent DNA. Because the level of H4K5Ac and H4K12Ac decrease as a replication fork progresses (Figure 4A), these acetylated sites specifically indicate the nascent chromatin. On the nascent DNA, PCNA unloading must be coordinated with nucleosome organization. H4K5Ac and H4K12Ac may be docking sites for chromatin-binding proteins that bridge PCNA unloading and chromatin status. We propose that the BRD4-ATAD5 complex is involved in cross-talk with the histone acetylation to fine-tune PCNA unloading. BRD4 was located to nascent DNA via recognizing acetylated histones (Figures 9). ATAD5 is also recruited to nascent DNA (Figures 4A). It remains to be elucidated how ATAD5 is recruited to the sites of DNA synthesis. BRD4 binding is not regarded to be necessary for the recruitment of ATAD5 to nascent DNA. Once there, BRD4 binds to ATAD5-RLC and interfere with PCNA unloading (Figures 9 and 10). As a replication fork proceeds, H4K5Ac and H4K12Ac undergo de-acetylation, and BRD4 is discharged from the nascent chromatin. The dissociation of BRD4 can trigger ATAD5-RLC for PCNA unloading. It has been reported that ATAD5-RLC is released from DNA with PCNA during unloading (Kang et al., 2019). While ATAD5-RLC is inhibited, PCNA remains on nascent DNA and supports the early steps of nascent chromatin assembly. Our study provides interesting perspective how epigenetic control affects the activity of replication machinery on nascent DNA.

REFERENCES

1. Kang, M. S., Kim, J., Ryu, E., Ha, N. Y., Hwang, S., Kim, B. G., Ra, J. S., Kim, Y. J., Hwang, J. M., Myung, K., & Kang, S. (2019). PCNA Unloading Is Negatively Regulated by BET Proteins. Cell reports, 29(13), 4632–4645.
2. Kang, S., Kang, M.S., Ryu, E., and Myung, K. (2018). Eukaryotic DNA replication: orchestrated action of multi-subunit protein complexes. Mutat. Res. 809, 58–69.
3. Moldovan, G.L., Pfander, B., and Jentsch, S. (2007). PCNA, the maestro of the replication fork. Cell 129, 665–679.
4. Shibahara, K., and Stillman, B. (1999). Replication-dependent marking of DNA by PCNA facilitates CAF-1-coupled inheritance of chromatin. Cell 96, 575–585.
5. Zhang, Z., Shibahara, K., and Stillman, B. (2000). PCNA connects DNA replication to epigenetic inheritance in yeast. Nature 408, 221–225.
6. Poot, R.A., Bozhenok, L., van den Berg, D.L., Steffensen, S., Ferreira, F., Grimaldi, M., Gilbert, N., Ferreira, J., and Varga-Weisz, P.D. (2004). The Williams syndrome transcription factor interacts with PCNA to target chromatin remodeling by ISWI to replication foci. Nat. Cell Biol. 6, 1236–1244.
7. Chen, J., Bozza, W., & Zhuang, Z. (2011). Ubiquitination of PCNA and its essential role in eukaryotic translesion synthesis. *Cell biochemistry and biophysics*, *60*(1-2), 47–60.
8. Kang, M.-S., Ryu, E., Lee, S.-W., Park, J., Ha, N.Y., Ra, J.S., Kim, Y.J., Kim, J., Abdel-Rahman, M., Park, S.H., et al. (2019). Regulation of PCNA cycling on replicating DNA by RFC and RFC-like complexes. Nat. Commun. 10, 2420.
9. Lee, K.Y., Fu, H., Aladjem, M.I., and Myung, K. (2013). ATAD5 regulates the lifespan of DNA replication factories by modulating PCNA level on the chromatin. J. Cell Biol. 200, 31–44.
10. Kurat, C.F., Yeeles, J.T.P., Patel, H., Early, A., and Diffley, J.F.X. (2017). Chromatin Controls DNA Replication Origin Selection, Lagging-Strand Synthesis, and Replication Fork Rates. Mol. Cell 65, 117–130.
11. Petryk, N., Dalby, M., Wenger, A., Stromme, C.B., Strandsby, A., Andersson, R., and Groth, A. (2018). MCM2 promotes symmetric inheritance of modified histones during DNA replication. Science 361, 1389–1392.
12. Reveron-Gomez, N., Gonzalez-Aguilera, C., Stewart-Morgan, K.R., Petryk, N., Flury, V., raziano, S., Johansen, J.V., Jakobsen, J.S., Alabert, C., and Groth, A. (2018). Accurate Recycling of Parental Histones Reproduces the Histone Modification Landscape during DNA Replication. Mol. Cell 72, 239–249e.5.
13. Yu, C., Gan, H., Serra-Cardona, A., Zhang, L., Gan, S., Sharma, S., Johansson, E., Chabes, A., Xu, R.M., and Zhang, Z. (2018). A mechanism for preventing asymmetric histone segregation onto replicating DNA strands. Science 361, 1386–1389.

14. Loyola, A., Bonaldi, T., Roche, D., Imhof, A., and Almouzni, G. (2006). PTMs on H3 variants before chromatin assembly potentiate their final epigenetic state. Mol. Cell 24, 309–316.
15. Sobel, R.E., Cook, R.G., Perry, C.A., Annunziato, A.T., and Allis, C.D. (1995). Conservation of deposition-related acetylation sites in newly synthesized histones H3 and H4. Proc. Natl. Acad. Sci. USA 92, 1237–1241.
16. Donati, B., Lorenzini, E., and Ciarrocchi, A. (2018). BRD4 and cancer: going beyond transcriptional regulation. Mol. Cancer 17, 164.
17. Jones, D.H., and Lin, D.I. (2017). Amplification of the NSD3-BRD4-CHD8 pathway in pelvic high-grade serous carcinomas of tubo-ovarian and endometrial origin. Mol. Clin. Oncol. 7, 301–307.
18. Konuma, T., Yu, D., Zhao, C., Ju, Y., Sharma, R., Ren, C., Zhang, Q., Zhou, M.M., and Zeng, L. (2017). Structural Mechanism of the Oxygenase JMJD6 Recognition by the Extraterminal (ET) Domain of BRD4. Sci. Rep. 7, 16272.
19. Liu, W., Ma, Q., Wong, K., Li, W., Ohgi, K., Zhang, J., Aggarwal, A., and Rosenfeld, M.G. (2013). Brd4 and JMJD6-associated anti-pause enhancers in regulation of transcriptional pause release. Cell 155, 1581–1595.
20. Shen, C., Ipsaro, J.J., Shi, J., Milazzo, J.P., Wang, E., Roe, J.S., Suzuki, Y., Pappin, D.J., Joshua-Tor, L., and Vakoc, C.R. (2015). NSD3-Short Is an Adaptor Protein that Couples BRD4 to the CHD8 Chromatin Remodeler. Mol. Cell 60, 847–859.
21. Zhang, Q., Zeng, L., Shen, C., Ju, Y., Konuma, T., Zhao, C., Vakoc, C.R., and Zhou, M.M. (2016). Structural Mechanism of Transcriptional Regulator NSD3 Recognition by the ET Domain of BRD4. Structure 24, 1201–1208.
22. Jang, M.K., Mochizuki, K., Zhou, M., Jeong, H.S., Brady, J.N., and Ozato, K. (2005). The bromodomain protein Brd4 is a positive regulatory component of P-TEFb and stimulates RNA polymerase II-dependent transcription. Mol. Cell 19, 523–534.
23. Yang, Z., Yik, J.H., Chen, R., He, N., Jang, M.K., Ozato, K., and Zhou, Q. (2005). Recruitment of P-TEFb for stimulation of transcriptional elongation by the bromodomain protein Brd4. Mol. Cell 19, 535–545.
24. Sansam, C.G., Pietrzak, K., Majchrzycka, B., Kerlin, M.A., Chen, J., Rankin, S., and Sansam, C.L. (2018). A mechanism for epigenetic control of DNA replication. Genes Dev. 32, 224–229.
25. Maruyama, T., Farina, A., Dey, A., Cheong, J., Bermudez, V.P., Tamura, T., Sciortino, S., Shuman, J., Hurwitz, J., and Ozato, K. (2002). A mammalian bromodomain protein, brd4, interacts with replication factor C and inhibits progression to S phase. Mol. Cell. Biol. 22, 6509–6520.

26. Gali, V.K., Dickerson, D., Katou, Y., Fujiki, K., Shirahige, K., Owen-Hughes, T., Kubota, T., and Donaldson, A.D. (2018). Identification of Elg1 interaction partners and effects on post-replication chromatin re-formation. PLoS Genet. 14, e1007783.
27. Crowe, B.L., Larue, R.C., Yuan, C., Hess, S., Kvaratskhelia, M., and Foster, M.P. (2016). Structure of the Brd4 ET domain bound to a C-terminal motif from g-retroviral integrases reveals a conserved mechanism of interaction. Proc. Natl. Acad. Sci. USA 113, 2086–2091.
28. Lee, K.B., Hwang, J.M., Choi, I.S., Rho, J., Choi, J.S., Kim, G.H., Kim, S.I., Kim, S., and Lee, Z.W. (2011). Direct monitoring of the inhibition of protein-protein interactions in cells by translocation of PKCd fusion proteins. Angew. Chem. Int. Engl. 50, 1314–1317.
29. Filippakopoulos, P., Qi, J., Picaud, S., Shen, Y., Smith, W.B., Fedorov, O., Morse, E.M., Keates, T., Hickman, T.T., Felletar, I., et al. (2010). Selective inhibition of BET bromodomains. Nature 468, 1067–1073.
30. Kuo, A.J., Song, J., Cheung, P., Ishibe-Murakami, S., Yamazoe, S., Chen, J.K., Patel, D.J., and Gozani, O. (2012). The BAH domain of ORC1 links H4K20me2 to DNA replication licensing and Meier-Gorlin syndrome. Nature 484, 115–119.
31. Azmi, I.F., Watanabe, S., Maloney, M.F., Kang, S., Belsky, J.A., MacAlpine, D.M., Peterson, C.L., and Bell, S.P. (2017). Nucleosomes influence multiple steps during replication initiation. eLife 6, e22512.
32. Shaila Rahman, Mathew E. Sowa, Matthias Ottinger, Jennifer A. Smith, Yang Shi, J. Wade Harper, Peter M. Howley. (2011). The Brd4 Extraterminal Domain Confers Transcription Activation Independent of pTEFb by Recruiting Multiple Proteins, Including NSD3. Molecular and Cellular Biology, 31 (13) 2641-2652.
33. Korb, E., Herre, M., Zucker-Scharff, I., Gresack, J., Allis, C.D., and Darnell, R.B. (2017). Excess Translation of Epigenetic Regulators Contributes to Fragile X Syndrome and Is Alleviated by Brd4 Inhibition. Cell 170, 1209–1223.e20.
34. Sun, C., Yin, J., Fang, Y., Chen, J., Jeong, K.J., Chen, X., Vellano, C.P., Ju, Z., Zhao, W., Zhang, D., et al. (2018). BRD4 Inhibition Is Synthetic Lethal with PARP Inhibitors through the Induction of Homologous Recombination Deficiency. Cancer Cell 33, 401–416.e8.
35. White, M.E., Fenger, J.M., and Carson, W.E., 3rd. (2019). Emerging roles of and therapeutic strategies targeting BRD4 in cancer. Cell. Immunol. 337, 48–53.
36. Huang, F., Saraf, A., Florens, L., Kusch, T., Swanson, S. K., Szerszen, L. T., Li, G., Dutta, A., Washburn, M. P., Abmayr, S. M., & Workman, J. L. (2016). The Enok acetyltransferase complex interacts with Elg1 and negatively regulates PCNA unloading to promote the G1/S transition. *Genes & development*, *30*(10), 1198–1210.
37. Sirbu, B.M., Couch, F.B., Feigerle, J.T., Bhaskara, S., Hiebert, S.W., and Cortez, D. (2011). Analysis of protein dynamics at active, stalled, and collapsed replication forks. Genes Dev. 25, 1320–1327.